Journal of Electron Spectroscopy and Related Phenomena 78 (1996) 203–208

XMCD Measurements in a high T_C molecular based magnet

M.-A. Arrio[a], Ph. Sainctavit[a,b], Ch. Cartier dit Moulin[b], Ch. Brouder[b,c], F.M.F. de Groot[b], T. Mallah[d] and M. Verdaguer[d]

[a]Laboratoire de Minéralogie-Cristallographie, CNRS URA9, Universités Paris VI et VII, 4 place Jussieu, 75252 Paris Cedex 05, France

[b]Laboratoire pour l'Utilisation du Rayonnement Electromagnétique, Bât. 209d, CNRS-CEA-MEN, 91405 Orsay Cedex, France

[c]Laboratoire de Physique du Solide de Nancy, CNRS URA155, BP239, 54506 Vandœuvre-lès- Nancy, France

[d]Laboratoire de Chimie des Métaux de Transition, CNRS URA419, Université Paris VI, 4 place Jussieu, 75252 Paris, France

The molecular based magnet $Cs^I[Ni^{II}Cr^{III}(CN)_6].2H_2O$ is a ferromagnet with a Curie temperature $T_C = 90$ K. Its structure consists of face centred cubic lattice of Ni^{II} ions connected by $Cr(CN)_6$ entities. We have recorded X-ray Magnetic Circular Dichroism (XMCD) at nickel $L_{2,3}$ edges. It clearly evidences that nickel II is in a high spin configuration and ferromagnetically coupled to the surrounding Cr^{III}. Through Crystal Field Multiplet calculations, we have determined the precise ground state of Ni^{II}. Special attention has been paid to the magnetic anisotropy that complicates the calculation of the cross section for a powder. By using sum rules derived for XMCD, it has been possible to extract the orbital and spin contributions to the total magnetic moment. A too small magnetic moment is found on nickel. A complete calculation taking into account the multiplet coupling effect and the covalent hybridisation showed that hybridisation cannot be responsible for the experimental low nickel magnetic moment. The origin of this effect is discussed.

1. INTRODUCTION

Conventional techniques in magnetism measure total magnetic moment (susceptibility measurements by SQUID, Faraday balance). Other more sophisticated techniques such as polarised neutron diffraction can give information on specific groups of atoms but measurements are only possible on large single crystals. X-ray Magnetic Circular Dichroism (XMCD) is a new technique that has recently received a strong interest by the community of magnetism. Magnetic Circular Dichroism has long been known in the energy range of visible light but was not investigated in the X-ray range due to the lack of sources of circular polarised X-rays. The development of Synchrotron Radiation in the last decade impulsed the field of X-ray spectroscopies and XMCD was first observed in 1987.[1]

In the second section we present the magnetic properties of the molecular based magnet and the third one is a basic summary of XMCD sum rules. The fourth section is dedicated to the experimental measurements and the fifth one outlines the results concerning the magnetic properties of the magnet.

2. MOLECULAR BASED MAGNETS

We have studied $Cs^I[Ni^{II}Cr^{III}(CN)_6].2H_2O$, a new type of magnets from inorganic chemistry. This magnet belongs to the family of bimetallic cyanides whose general formulae are $Cs^I[A^{II}B^{III}(CN)_6].nH_2O$ where A and B are 3d transition metal ions. It is synthesized through soft chemistry engineering at room temperature.[2] The structure of $Cs^I[Ni^{II}Cr^{III}(CN)_6].2H_2O$ consists of a three-dimensional assembly of structural motifs -N≡C-Cr-C≡N-Ni- where the metallic cations are arranged in a rock salt lattice.[2] The Ni^{II} ions are surrounded by six nitrogen atoms and the Cr^{III} ions by six carbon atoms. Both have an octahedral symmetry. Caesium

0368-2048/96/$15.00 © 1996 Elsevier Science B.V. All rights reserved
PII S0368-2048 (96) 02713-2

ions are present in half of the tetrahedral sites and two water molecules are present per formula unit. Using powder X-ray diffraction we found that the compound is pure and well crystallized with the cell parameter a = 10.57 Å[2]. From infra-red spectroscopy, it can be inferred that no Ni^{II} are coordinated to carbon atoms of the cyano bridges.

In $Cs^{I}[Ni^{II}Cr^{III}(CN)_6].2H_2O$, an orbital interpretation based on the model of Kahn et al.[3] allows to foresee a short-range ferromagnetic interaction between the two ions. In that model, the three unpaired electrons of Cr^{III} (d^3) are described by t_{2g} orbitals partially delocalized on the π system of cyanides and particularly on p_π orbitals of the nitrogen atoms. The two unpaired electrons of Ni^{II} (d^8) are described by e_g orbitals partially delocalized on the surrounding nitrogen atoms (p_σ orbitals). It results a strict orthogonality between the two kinds of orbitals of different symmetry : t_{2g} for Cr^{III} and e_g for Ni^{II}. Furthermore, the delocalization of the t_{2g} (Cr^{III}) orbitals and the e_g (Ni^{II}) on the nitrogen atoms allows a strong overlap density t_{2g}-e_g on the nitrogen atom ; the large value of the bielectronic exchange integrals governs the value of the ferromagnetic short range interaction, reflected in the high Curie temperature (T_C = 90 K).

The magnetic properties of the compound have been thoroughly measured by conventional techniques. From magnetization curves, the saturation moment at 3 tesla is found to be 5.2 μ_B per molecular unit at 3 K. This is consistent with the two Bohr magnetons carried by nickel and the three by chromium. This is also supported by the magnetic susceptibility measurements at high temperature. Field cooled magnetization measurements at 10 G clearly evidence that the Curie temperature is 90 K. Hysteresis loop shows that the remnant magnetic moment is 1.5 μ_B per formula unit with a coercive field of 80 G : $Cs^{I}[Ni^{II}Cr^{III}(CN)_6].2H_2O$ is indeed a magnet.[2]

Neutron diffraction with non spin polarized neutrons has been performed on powdered samples.[3] Diffractograms have been registered above and below the Curie temperature. The difference between the two diffractograms has been analyzed. The difference amounts to 2 % of the average signal. From the absence of super-structure peaks (nickel and chromium are coupled ferromagnetically) it can be inferred that the magnetic moment carried by nickel and chromium are not much different, leading for the nickel moment to a value somewhat higher than 2 μ_B. No refinement on the difference signal could be made because of the small number of peaks for a cubic powder and the poor quality of the signal/noise ratio.

From combined EPR measurements on the magnet $Cs^{I}[Ni^{II}Cr^{III}(CN)_6].2H_2O$ and $Zn^{II}_3[Cr^{III}(CN)_6]_2.xH_2O$ we have determined the effective Landé factor of Ni^{II}. We found g_{Ni} = 2.15 ± 0.02, from which we deduce that $\frac{<L_z>}{<S_z>}$ = 0.15 ± 0.02.

3. XAS AND XMCD

During the absorption process the atom undergoes a transition from an initial state to a final state and when the absorption cross section is expressed in the electric dipole approximation the interaction Hamiltonian reads $\vec{\varepsilon}.\vec{r}$ where $\vec{\varepsilon}$ the polarization vector characterizing the photon beam. XMCD is performed when the cross section of a magnetic sample is registered for circularly polarized light. The XMCD signal is the difference between the two cross sections for left ($\vec{\varepsilon}.\vec{r} = \frac{x+iy}{\sqrt{2}}$) and right ($\vec{\varepsilon}.\vec{r} = \frac{-x+iy}{\sqrt{2}}$) circularly polarized light.

We have measured $L_{2,3}$ edges of nickel. The main channel corresponds to a transition from the initial state $2p^63d^8$ to the final state $2p^53d^9$. The channel that corresponds to transitions toward continuum s states is ignored since it is commonly found negligible.[4] By definition the cross sections are labelled σ_0 for linear polarization parallel to the magnetic field, σ_+ for left circular polarization and σ_- for right circular polarization (in both circular polarization, the propagation vector is parallel to the magnetic field).

Thole and Carra et al.[5] have developed several sum rules that can be applied to XMCD spectra. The orbital sum rules at $L_{2,3}$ edges for electric dipole transitions read

$$\frac{I^+_{2,3} - I^-_{2,3}}{I^+_{2,3} + I^-_{2,3} + I^0_{2,3}} = -\frac{<\phi_i|L_z|\phi_i>}{2(10-n)} \quad (1)$$

where n is the occupation number of the 3d orbital (n=8 for Ni^{II}), $|\phi_i>$ the Ni^{II} ground state, I^+_3 the integral of the absorption cross section over the L_3

edge for left polarized photons and similar definitions for others I. The +, -, 0 indices relate respectively to left, right, linear polarization and we use $I^+_{2,3} = I^+_3 + I^+_2$. The spin sum rule reads

$$\frac{(I^+_3 - I^-_3) - 2(I^+_2 - I^-_2)}{I^+_{2,3} + I^-_{2,3} + I^0_{2,3}} = -\frac{2}{3(10-n)}\left[\langle\phi_i|S_z|\phi_i\rangle + \frac{7}{2}\langle\phi_i|T_z|\phi_i\rangle \right] \quad (2)$$

The I values can be computed from the experimental data ($I = \int \frac{\sigma}{h\nu} d(h\nu)$), so that direct determinations of $\langle S_z\rangle$ and $\langle L_z\rangle$ are possible from experimental data. From these sum rules, one gets $\langle L_z\rangle$ and $\langle S_z\rangle$ (after evaluating $\langle T_z\rangle$ as discussed later) hence also the magnetic moment $M = -\mu_B\langle L_z+2S_z\rangle$ carried by the absorbing atom.

4. MEASUREMENTS AT Ni $L_{2,3}$ EDGES

We measured XMCD at nickel $L_{2,3}$ edges in the molecular-based magnet $Cs^I[Ni^{II}Cr^{III}(CN)_6].2H_2O$ on the soft X-ray SU22 beam line of the storage-ring Super-ACO at LURE (Orsay). The spectra are registered in total electron yield and the instrumental broadening at nickel $L_{2,3}$ edges has been measured to be 0.25 eV. The applied magnetic field is usually 1 Tesla. We have computed the circular polarization transfer function of Beryl crystals in the framework of the dynamical theory. We find that the polarization rate, τ, is 37.1 % at L_3 edge (853 eV) and 30.9 % at L_2 edge (870.3 eV).[6] More experimental details can be found elsewhere.[7]

During a XMCD experiment, a first spectrum, labelled $\sigma_{\uparrow\uparrow}$, is registered with the magnetic field parallel to the propagation vector of the photons. Then a second spectrum, labelled $\sigma_{\uparrow\downarrow}$, is registered with the magnetic field anti-parallel to the propagation vector of the photons. $\sigma_{\uparrow\uparrow}$ and $\sigma_{\uparrow\downarrow}$ depend on τ and are related to σ_+ and σ_- through $\sigma_{\uparrow\uparrow} = \frac{\tau+1}{2}\sigma_+ + \frac{1-\tau}{2}\sigma_-$ and $\sigma_{\uparrow\downarrow} = \frac{1-\tau}{2}\sigma_+ + \frac{\tau+1}{2}\sigma_-$. It can be shown that, in the electric dipole approximation, reversing the magnetic field is equivalent to changing the helicity of the beam. The XMCD signal is the difference $(\sigma_{\uparrow\uparrow} - \sigma_{\uparrow\downarrow})$ between the two spectra. Since the XMCD signal is obtained by difference between two spectra that are not registered at the same time, great care is needed in the normalization process : we checked that the two spectra registered with fully linearly polarized light for two directions of the magnetic field differ by a constant multiplication factor equal to 1.1. We used the same factor to normalized $\sigma_{\uparrow\uparrow}$ and $\sigma_{\uparrow\downarrow}$ spectra. All the experiments have also been performed above and bellow the orbit plane and yielded the same although reversed, dichroic signal.

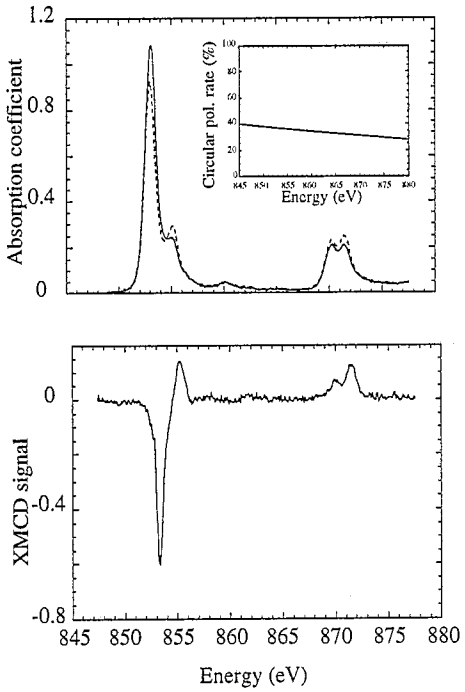

Figure 1. Top: $\sigma_{\uparrow\uparrow}$ (line) and $\sigma_{\uparrow\downarrow}$ (dash) at nickel $L_{2,3}$ edges. Bottom, XMCD signal $\sigma_{\uparrow\downarrow} - \sigma_{\uparrow\uparrow}$ normalized to 100 % of circular polarization. The energy dependent circular polarization rate is plotted in insert.

5. RESULTS AND DISCUSSION

The two spectra $\sigma_{\uparrow\uparrow}$ and $\sigma_{\uparrow\downarrow}$ at nickel $L_{2,3}$ edges are plotted in figure 1. Each spectrum is the sum of six spectra for each direction of the magnetic field, with an accumulation time of one second per point. Although the samples are insulating compounds and the photo current is low, a very good signal/noise ratio can be obtained. The spectra are characteristic of Ni^{II} in the triplet state as can be confirmed by the multiplet calculations. The net magnetic moment of the sample is parallel to the magnetic moment of chromium (around $3\mu_B$) and the sign of the

experimental XMCD signal proves that nickel (II) ions are indeed coupled ferromagnetically to chromium (III) ions.

To simulate the spectra, we have calculated the cross sections in the Ligand Field Multiplet Theory.[8] It takes into account spin-orbit coupling and treats the environment of the absorbing atom through crystal field parameters. In octahedral symmetry, the crystal field strength is determined by the average energy separation between t_{2g} and e_g, commonly labelled 10Dq. The parameter is determined by UV-visible electronic spectroscopy and equals to ≈ 1.3 eV around the nickel ions. In the model we have used only the two configurations $3d^8$ and $3d^9\underline{L}$ for Ni^{II} ground state and related configurations for the excited state.

Magnetic anisotropy

The sample is a powder of crystallites with cubic crystallographic symmetry. Without magnetic field the electric dipole cross sections are isotropic for any crystallites. When a magnetic field is applied, the presence of a net magnetization of the sample breaks the cubic symmetry in each crystallite. Due to magnetic anisotropy the break of cubic symmetry depends on the orientation of the magnetic field with respect to the crystallographic axes of the crystallites. To take into account this effect, the powder spectrum has to be calculated by averaging cross sections for all possible directions of magnetization respectively to the symmetry axes of the crystallites. Since the complete calculation would be intractable, we used the approximate method of integration developed by Ayant et al.[9] It states that the powder cross section can be obtained to a good approximation by a well-balanced average of cross sections calculated with particular directions of the magnetic field. In the case of cubic symmetry, the powder spectrum is given by :

$$\sigma_{powder} = \frac{176}{385}\sigma(B//C_2) + \frac{99}{385}\sigma(B//C_3) + \frac{110}{385}\sigma(B//C_4)$$

where $\sigma(B//C_2)$, $\sigma(B//C_3)$ and $\sigma(B//C_4)$ are the cross sections corresponding to the magnetic field B parallel to the following directions : [110] or C_2, [111] or C_3 and [001] or C_4. We performed the multiplet calculations for a magnetic field parallel to C_2, C_3 and C_4. The isotropic spectra for any of the three directions are very similar as can be expected since the Zeeman Hamiltonian is a small perturbation that cannot be resolved by the experimental resolution. On the contrary when linear or circular dichroism is calculated large differences are present due to different degeneracy lift and different dipole allowed transitions. This proves that a well balanced averaging procedure is essential to allow the extraction of physical quantities from the comparison between experimental and calculated $\frac{1}{2}(\sigma_+ + \sigma_-)$ spectra (Fig.2).

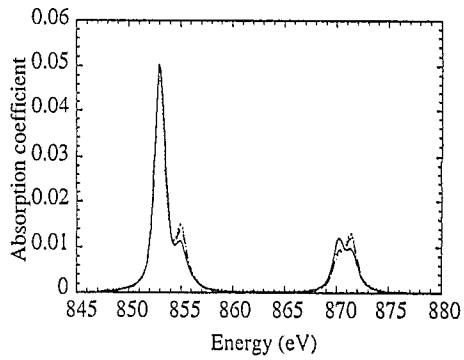

Figure 2. Ni^{II} $L_{2,3}$ edges theoretical spectra $\frac{1}{2}(\sigma_+ + \sigma_-)$ for different magnetic field **B** directions. : Dashed line: **B**//C_2(110). Dots: **B**//C_3(111) dots; solid line: **B**//C_4(100).

The crystal field and spin orbit parameters are adjusted to produce the best agreement between the experimental and the powdered averaged theoretical cross section $\frac{1}{2}(\sigma_+ + \sigma_-)$. The calculation is performed at 0 K and the best agreement is obtained for spin-orbit parameters ζ_{2p} = 11.4 eV and ζ_{3d} = 0.1 eV, a crystal field parameter 10Dq = 1.4 eV in agreement with the one obtained by optical spectroscopy. We used Δ = 5.3 eV, U_{cd}-U_{dd} = 1 eV, $V(e_g)$ = 2 and $V(t_{2g})$ = -1 (we keep the notations by Kotani[10]). Figure 3 compares experimental and theoretical $\frac{1}{2}(\sigma_+ + \sigma_-)$ spectra. The general shape of the experimental $\frac{1}{2}(\sigma_+ + \sigma_-)$ as well as the satellite at 850 eV are well reproduced by the calculation.

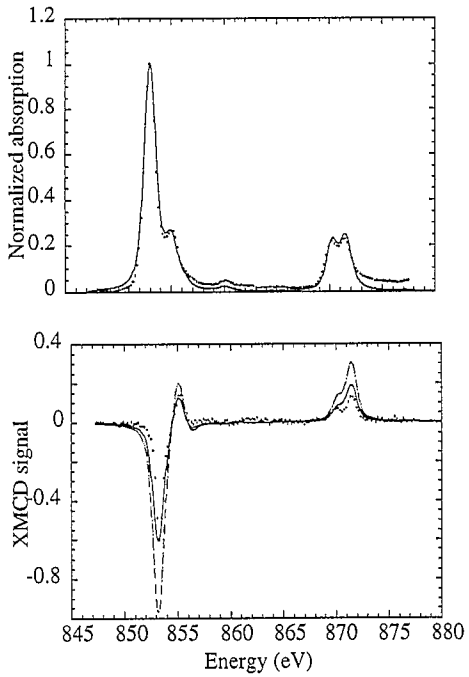

Figure 3. Top, experimental (dots) and theoretical (line) $\frac{1}{2}(\sigma_+ + \sigma_-)$ spectra. Bottom, experimental (dots), theoretical (dash) and theoretical divided by 1.6 XMCD signals.

We find that the Ni^{II} ground state is a mixture of $3d^8$ that counts for 90 % and of $d^9\underline{L}$ that counts for 10 %. This result shows that Ni^{II} has a very ionic character compared to the values obtained by Kotani for a set of Ni^{II} compounds.[10] On figure 3, we have also plotted experimental and calculated XMCD spectra. The shape of the XMCD signal is well reproduced by the calculation except for the amplitude that is 1.6 times larger than the experimental one. The application of Eq.1 to the experimental spectra gives $M_L = -\langle L_z\rangle\mu_B = 0.1\mu_B \pm 0.03\mu_B$ and where $\mu_B > 0$. Although the crystal field parameter is large, the orbital momentum is not completely quenched. This originates from the deviation of the ground state from the pure $^3A_{2g}$ state. As stated above the computation of $\langle S_z\rangle$ through the spin sum rule requires the knowledge of the average value of the spherical tensor T_z. We calculated $\langle T_z\rangle$ for Ni^{II} ground state and we found $\langle T_z\rangle = 0.0017$. From the application of the spin sum rule (Eq.2) to the experimental spectra, we obtained $M_S = -2\langle S_z\rangle\mu_B = 0.78\ \mu_B$ if we neglect $\langle T_z\rangle$ and $M_S = -2\langle S_z\rangle\mu_B = 0.80\ \mu_B$ if we take into account $\langle T_z\rangle$. In the case of Ni^{II}, the error induced by neglecting $\langle T_z\rangle$ is not large, it is less than 3% of the total magnetic moment. The total magnetic moment on Ni^{II} is found equal to $M = -[\langle L_z\rangle + 2\langle S_z\rangle]\mu_B = 0.9\ \mu_B \pm 0.1\ \mu_B$ per absorbing Ni^{II} ion. The error on the determination of $\langle L_z\rangle$ and $\langle S_z\rangle$ is mainly related to the uncertainty of circular polarization rate (10 %). For $\langle L_z\rangle$ it is somewhat larger than 10 % because L_2 and L_3 dichroic signals tend to cancel and systematic errors can occur from normalization process. The Ni^{II} magnetic moment extracted from XMCD measurements is lower than the one ($\approx 2\ \mu_B$) expected for a fully magnetized Ni^{II} atom in $^3A_{2g}$ triplet state.

A possible origin for the loss of magnetic moment could be hybridization between Ni^{II} ions and the neighbouring nitrogen atoms. In the Ligand Field Multiplet model, Ni^{II} states are represented by a mixture of the two electronic configurations $3d^8$ and $3d^9\underline{L}$, where $d^9\underline{L}$ is a configuration where an extra electron coming from the ligand orbitals is added on the 3d shell. One finds by applying the sum rules to the theoretical spectra that both M_L and M_S are not much affected by hybridization : taking $n = 8.1$ in Eqs.1-2 and neglecting $\langle T_z\rangle$, we find $M_L = 0.2_7\ \mu_B$ and $M_S = 1.8\ \mu_B$. The covalence tends to decrease the total magnetic moment by less than 10 % and most of this effect comes from the variation of 3d holes number between pure $3d^8$ and $3d^8$–$3d^9\underline{L}$ mixture.

An explanation for the low value of the XMCD Ni magnetic moment could be related to an incomplete magnetization of the Nickel atoms. We performed at 20 K a XMCD measurement with an external magnetic field of 5 tesla and found that the XMCD signal had the same amplitude as for the 1 tesla experiment to less than 5% relative error. Then one can safely consider that any bulk Ni^{II} ion has reached full magnetization in our experiments performed at 20 K with 1 tesla magnetic field. Nevertheless since total electron yield detection is surface sensitive, surface nickel ions might not be feeling the exchange magnetic field or strong magnetic anisotropy may be present making the magnetization perpendicular to the surface negligible. This hypothesis cannot be discarded.

From XMCD, the experimental value for $\frac{<L_z>}{<S_z>}$ is $0.2_6 \pm 0.05$ and the theoretical value extracted from Ligand Field Multiplet Calculation is around $0.2_9 \pm 0.05$. EPR measurements have shown that $\frac{<L_z>}{<S_z>}$ in Ni^{II} should be around 0.15 ± 0.02. One sees that $\frac{<L_z>}{<S_z>}$ determination by our measurements is larger than the one determined by EPR. This effect supports the idea that Ni^{II} ions undergo a strong magnetic anisotropy and that $<L_z>$ and $<S_z>$ measurements do not refer to bulk magnetic Ni^{II} ions. This type of disagreement has already been mentioned by other authors who also found that $\frac{<L_z>}{<S_z>}$ extracted from XMCD is usually larger than the one extracted from other techniques.

6. CONCLUSION

We have studied the nickel $L_{2,3}$ edges in the bimetallic cyanide $Cs^I[Ni^{II}Cr^{III}(CN)_6].2H_2O$. We have been able to evidence a strong XMCD signal on the Ni^{II} in the bimetallic cyanide $Cs^I[Ni^{II}Cr^{III}(CN)_6].2H_2O$. We have calculated XAS and XMCD spectra in the Ligand Field Multiplet approach and we have shown that hybridization has to be introduced for a complete simulation of the experimental spectra. The $3d^9\underline{L}$ configuration weights for 10 % in Ni^{II} ground state and tends to decrease the spin and the orbital momentum. In doing the calculations, we particularly checked that T_z is negligible and calculated the magnetic anisotropy in a cubic crystal field.

Although experimental and calculated isotropic spectra agreed very well we found a serious underestimation of the magnetic moment extracted from XMCD sum rules compared the one that is expected for an almost pure triplet state for Ni^{II}. EPR measurements indicate that total electron yield measurements do not provide information on bulk magnetized ions and that surface anisotropy may be responsible for the incomplete saturation of Ni^{II} ions and large $<L_z>$ contribution relative to $<S_z>$. The low Ni 3d magnetic moment may be related to XMCD experiments at nickel K edge where a large 4p magnetic moment is found and to XMCD measurements at nitrogen K edge that have also shown that nitrogen atoms carry a weak magnetic moment[11]. Both results being confirmed by polarized neutron diffraction experiments and local density functional calculations.[12]

REFERENCES

1. Schütz, G.; Wagner, W.; Wilhelm, W.; Kienle, P.; Zeller, R.; Frahm, R.; Materlik, G. Phys. Rev. Lett. **1987**, 58, 737-740.
2. Gadet, V.; Mallah, T.; Castro, I.; Veillet, P.; Verdaguer, M. J. Am. Chem. Soc. **1992**, 114, 9213-9214.
3. Kahn, O.; Galy, O.; Journaux, Y.; Jaud, J.; Morgenstern-Badarau, I. J. Am. Chem. Soc. **1982**, 104, 2165.
4. Bianconi, A.; Della Longa, S.; Li, C.; Pompa, M.; Congiu-Castellano, A.; Udron, D.; Flank, A. M.; Lagarde, P. Phys. Rev. B **1991**, 44, 10126-10138.
5. Carra, P.; Thole, B.T.; Altarelli, M.; Wang, X. Phys. Rev. Lett. **1993**, 70, 694-697
6. Lefebvre, D.; Sainctavit, Ph.; Malgrange, C. Rev. Sci. Instrum. **1994**, 65, 2556-2561.
7. Sainctavit, Ph.; Lefebvre, D.; Cartier dit Moulin, Ch.; Laffon, C.; Brouder, Ch.; Krill, G.; Schillé, J.-Ph.; Kappler, J.-P.; Goulon J. J. Appl. Phys. **1992**, 72, 1985-1988.
8. van der Laan, G.; Kirkman, I.W. J. Phys.: Condens. Matter **1992**, 4,4189-4204
9. Ayant, Y.; Belorizky, E.; Guillot, M.; Rosset, J. Le Journal de Physique **1965**, 26, 7, 385-389.
10. Kotani, A.; Okada, K. Technical Report of ISSP **1992**, Ser. A, 2562.
11. Verdaguer, M.; Mallah, T.; Hélary, C.; L'Hermite, F.; Sainctavit, Ph.; Arrio, M.-A.; Babel, D.; Baudelet, F.; Dartyge, E.; Fontaine, A. Nucl. Instrum. Methods. B **1995**, 208, 765-767.
12. Figgis, B. N.; Kucharski, E. S.; Vrtis, M. J. Am. Chem. Soc. **1993**, 115, 176-181.